

Assessing the pre-seismic and post-seismic displacement in the Athens metropolitan area by SAR Interferometric Point Target Analysis, using ERS and ENVISAT datasets

Ioannis Papoutsis⁽¹⁾, Charalabos Kontoes⁽²⁾, Basil A. Massinas⁽¹⁾, Demitris Paradissis⁽¹⁾ and Panayiotis Frangos⁽³⁾

(1) National Technical University of Athens, Dionysos Satellite Observatory, Iroon Polytechniou 9, 15780, Zografou, Athens, Greece, ipapoutsis@space.noa.gr, billmass@central.ntua.gr, dempar@central.ntua.gr

(2) National Observatory of Athens, Institute for Space Applications and Remote Sensing, Vas. Pavlou & I. Metaxa, 15236, Penteli, Athens, Greece, kontoes@space.noa.gr

(3) National Technical University of Athens, School of Electrical and Computer Engineering, Iroon Polytechniou 9, 15780, Zografou, pfrangos@central.ntua.gr

ABSTRACT

This is a preliminary study of the deformation rate pattern observed in the Athens metropolitan area, by means of Interferometric Point Target Analysis, using ERS-1,2 SAR time series spanning from 1992 to 2001. The motivation behind this work laid in four main directions: (i) the production of a diachronic reference Point Target distribution map, (ii) the mapping of the displacement occurring in the Athens area that was induced by the intense construction activities and other geophysical phenomena in the preceding years and (iii) the identification of the small scale deformation field, which might be pre-cursor of future abrupt and destructive events. The analysis led to the identification of more than 130000 stable Point Targets. It was discovered that the area of Kifissia, located on the North of the Athens commercial center is undergoing significant subsidence of the order of 4-5 mm/year, most likely attributed to water pumping.

1. INTRODUCTION

Classic InSAR technique has offered a great deal of reliable measurements of ground deformation. The accuracy of this method though is limited by components related to spatial and temporal decorrelation, signal delay due to tropospheric and ionospheric disturbances, orbital errors as well as Digital Elevation Model (DEM) artifacts. These components are dealt with the well established Interferometric Point Target Analysis (IPTA) technique. The IPTA methodology offers significant improvement in estimating the near vertical displacement rates with accuracy higher than 1mm/year. Thus, this technique is ideal for measuring small-scale ground deformation due to seismic precursor activity, urban subsidence, creep

effects in fault zones as well as displacements in active fault zones and volcanoes.

2. ATHENS METROPOLITAN AREA

The city of Athens, shown in Fig. 1, is a densely populated urban Metropolis, covering about 200 Km². The socio-economic importance of the city is well known. Over the years a high seismic risk has been reported with the most severe event being the Athens earthquake held on September 7th, 1999 [1] with a large number of damages and human casualties. During the last decades an intense construction activity has taken place in the city. In the wide frame of the preparation of the Olympic Games 2004 in Athens, several major infrastructure projects like Eleftherios Venizelos International Airport, Athens sub-way, new tram lines, and highways have been realised. This construction activity together with old mining works and the geophysical phenomena reported (e.g. earthquakes, possible subsidence due to extended water pumping, shrink and swell of geological formations - especially clay-rich), dictate the city monitoring over the years.

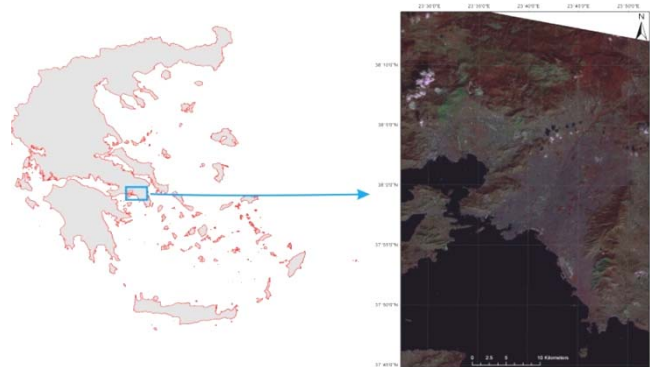


Figure 1. Location of the Athens Metropolitan area within Greece.

One of the most significant natural disasters which struck Greece in the 20th century was the 07/09/1999, 11^h 56^m 50^s UTC, Mw = 5.9 Athens earthquake. It claimed the lives of 143 people, and caused the collapse of several buildings mainly in the northwest suburbs of the Greek capital. The approximate location of the epicenter of the earthquake was 38.10°N, 23.56°E, roughly 20 km northwest from the center of Athens.

The vertical displacement field at surface level caused by this tectonic event, was investigated with space born Synthetic Aperture Radar Interferometry (InSAR), using ERS-2 data. The spatial pattern of the deformation induced from the catastrophic earthquake, along with measured displacement is shown in Fig. 2. InSAR processing revealed significant deformation with a maximum Line Of Sight (LOS) subsidence of approximately 6 cm [1]. This observation was used in earthquake modeling and fault location mapping in the middle of the mountain Parnitha. The region of maximum deformation coincided with the main shock epicenter and this was validated through leveling measurements across the Mornos river open aqueduct, used for water supply in Athens [2].

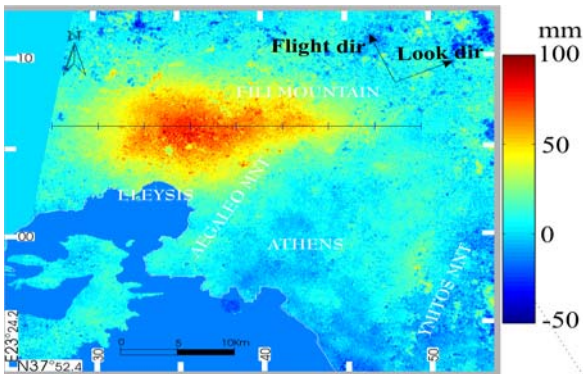


Figure 2. Unwrapped co-seismic interferogram of the 7/9/1999 Athens earthquake.

3. DATA USED

For implementing Interferometric Point Target Analysis (IPTA) a large dataset of SAR scenes is required. Hence, in the frame of ESA-GREECE AO project 1489OD/11-2003/72, more than 70 ERS-1,2 and ENVISAT scenes were obtained for further processing. The track number was 465, frame 2835. Tab. 1 presents the dataset for ERS-1, 2 and ENVISAT.

Table 1. ERS-1,2 and ENVISAT dataset.

No	Orbit	Date	Sensor	No	Orbit	Date	Sensor
1	07123	92-11-25	ERS1	1	04026	02-07-12	ENVISAT
2	07624	92-12-30	ERS1	2	06030	03-04-26	ENVISAT
3	10129	93-06-23	ERS1	3	07032	03-07-05	ENVISAT
4	12133	93-11-10	ERS1	4	07533	03-08-09	ENVISAT
5	20493	95-06-16	ERS1	5	08535	03-10-18	ENVISAT
6	20994	95-07-21	ERS1	6	09036	03-11-22	ENVISAT
7	01321	95-07-22	ERS2	7	09537	03-12-27	ENVISAT
8	21495	95-08-25	ERS1	8	11040	04-04-10	ENVISAT
9	01822	95-08-26	ERS2	9	11541	04-05-15	ENVISAT
10	21996	95-09-29	ERS1	10	12042	04-06-19	ENVISAT
11	02323	95-09-30	ERS2	11	12543	04-07-24	ENVISAT
12	22497	95-11-03	ERS1	12	13044	04-08-28	ENVISAT
13	02824	95-11-04	ERS2	13	14046	04-11-06	ENVISAT
14	22998	95-12-08	ERS1	14	15048	05-01-15	ENVISAT
15	03325	95-12-09	ERS2	15	15549	05-02-19	ENVISAT
16	23499	96-01-12	ERS1	16	16551	05-04-30	ENVISAT
17	03826	96-01-13	ERS2	17	17052	05-06-04	ENVISAT
18	24501	96-03-22	ERS1	18	18054	05-08-13	ENVISAT
19	06331	96-07-06	ERS2	19	18555	05-09-17	ENVISAT
20	06832	96-08-10	ERS2	20	20058	05-12-31	ENVISAT
21	07333	96-09-14	ERS2	21	21060	06-03-11	ENVISAT
22	07834	96-10-19	ERS2	22	25569	07-01-20	ENVISAT
23	13846	97-12-13	ERS2	23	26070	07-02-24	ENVISAT
24	17353	98-08-15	ERS2	24	29577	07-10-27	ENVISAT
25	17854	98-09-19	ERS2	25	33585	08-08-02	ENVISAT
26	18355	98-10-24	ERS2	26	34086	08-09-06	ENVISAT
27	18856	98-11-28	ERS2	27	35589	08-12-20	ENVISAT
28	19858	99-02-06	ERS2	28	39096	09-08-22	ENVISAT
29	21361	99-05-22	ERS2	29	40098	09-10-31	ENVISAT
30	21862	99-06-26	ERS2				
31	22363	99-07-31	ERS2				
32	23866	99-11-13	ERS2				
33	24367	99-12-18	ERS2				
34	26872	00-06-10	ERS2				
35	27373	00-07-15	ERS2				
36	27874	00-08-19	ERS2				
37	28375	00-09-23	ERS2				
38	28876	00-10-28	ERS2				
39	29377	00-12-02	ERS2				
40	29878	01-01-06	ERS2				

4. MASTER SELECTION FOR THE ERS-1,2 DATASET

IPTA processing involves the selection of a common master scene to be used for forming the differential

interferograms. The most favorable master scene must encompass three main characteristics: (a) Uniform distribution of perpendicular baselines, (b) Reduced atmospheric signal contribution and (c) reduced combined temporal and geometrical decorrelation.

The latter criterion in the master selection process required the calculation of the expected coherence of the interferometric stack. This is done via Eq. 1 [3]:

$$\gamma^m = \frac{1}{K} \sum_{k=0}^K g(B_n^{k,m}, 1200) \times g(T^{k,m}, 5) \times g(f_{DC}^{k,m}, 1380), \quad (1)$$

$$g(x, c) = 1 - \frac{|x|}{c} \text{ if } |x| < c \text{ else } g(x, c) = 0$$

, where B_n is the perpendicular baseline, T is the temporal baseline and f_{DC} is the Doppler Centroid.

Using the above formulation, Fig.3 depicts the expected coherence for each of the scenes in the ERS-1,2 stack.

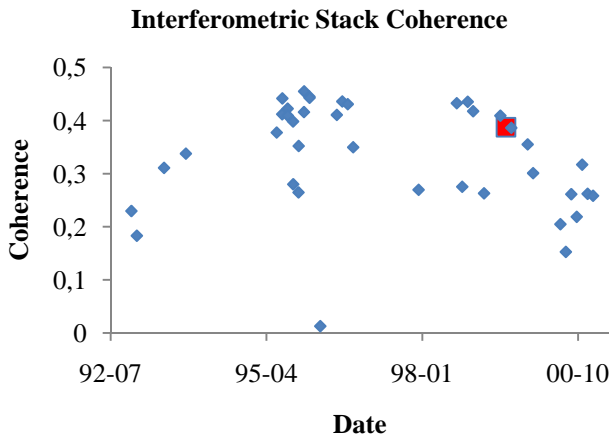


Figure 3. Expected coherence of the interferometric stack for each scene of the ERS-1,2 dataset. The red square corresponds to the selected master image.

Accounting for the criteria mentioned above, the scene with orbit No 21862, on 26/06/1999 was selected as a suitable master image that meets these requirements. The corresponding distribution of the baselines for this master scene is shown in Fig. 4, where it is evident that the perpendicular baseline sampling is satisfactory for the application of the IPTA processing chain.

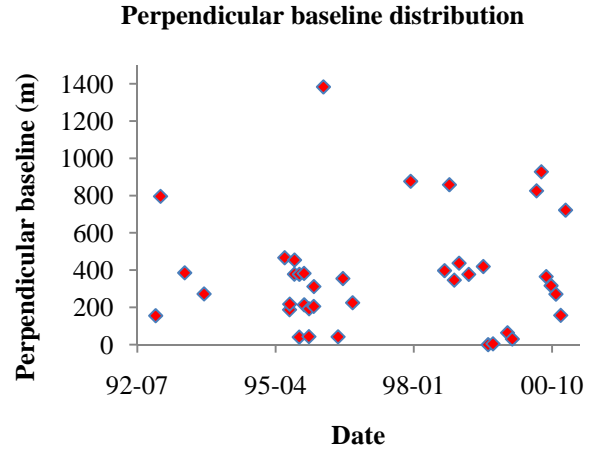


Figure 4. Perpendicular baseline distribution for the master scene with orbit No 21862.

5. INTERFEROMETRIC POINT TARGET ANALYSIS ON THE ERS-1,2 DATASET

Following the standard procedure, as the one proposed by *Ferretti et al.* in [4] the 39 scenes were accurately co-registered to the common master scene on a subpixel basis, achieving standard deviations of the order of 0.15 pixels on average. The generation of the differential interferograms was then straightforward, with the use of SRTM3 data for the Digital Elevation Model (DEM). Precision orbit files associated with each scene were extracted either from DELFT or from ESA DORIS, depending on data availability.

The next step was the selection of point candidates which do not change their scattering behavior over time. This was done through the calculation of the mean/sigma ratio, where mean is the temporal average of the backscattering signal and sigma is the standard deviation of the backscattering image from this average. The threshold for this ratio was set to 1.5. An additional method used for extracting stable point candidates, by exploiting the concept that a scatterer needs to dominate the clutter scattering in each image [5]. A factor of 1.0 was used as a threshold, which means that the candidate target backscattering has to be above the local spatial average. Merging the two criteria, more than 350000 point candidates were found for the Athens metropolitan area.

For the selected point candidates a regression analysis accounting for the linear component of the deformation velocity and for the DEM error was run. This first

estimate was then subtracted from the differential interferograms and the regression analysis was tested again. Through several iterations a first solution was derived. An intermediate step at this stage was the refinement of the baselines using the interferometric data, a procedure necessary to eliminate orbital errors that appear as coarse phase ramps in the interferograms. It should be mentioned that the iteration process is not an automatic procedure, since for every step there is a need for consistency checking of the result in terms of unwrapping errors.

Having reached a robust first solution, this was subsequently subtracted from the original differential interferograms. The remaining residuals corresponded to the atmospheric signal, to the non-linear component of the deformation signal and to noise. The atmospheric contribution was then estimated by taking advantage of its spatial correlation statistics, through spatial filtering. Fig. 5 shows the atmospheric signal of a certain scene of the dataset, where the spatial correlation is evident.

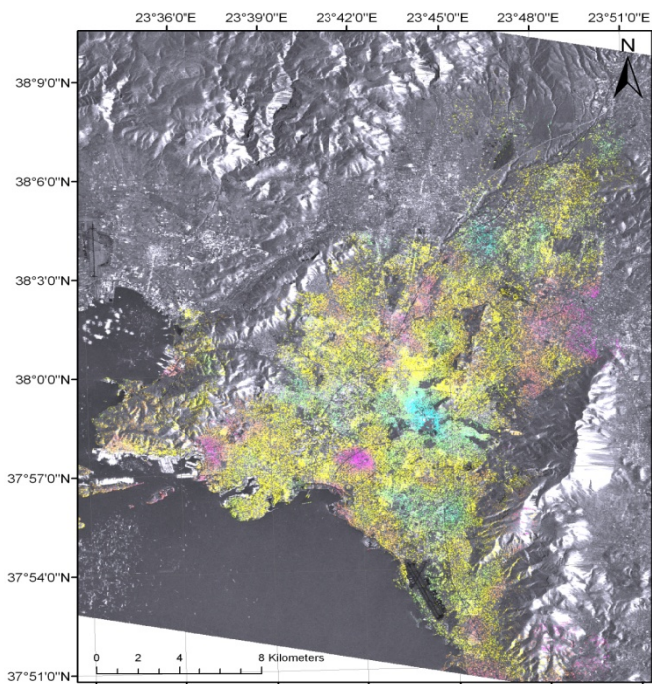


Figure 7. Atmospheric signal for scene with orbit No 20994, an intermediate product in the IPTA processing.

The second improved solution was obtained by subtracting the atmospheric phase from the interferograms and re-running the regression analysis. At this point the remaining residuals are mainly considered as non-linear deformation plus noise. For

every linear regression analysis iteration the number of accepted point targets was reduced according to the phase standard deviation from the regression fit which was used as a quality measure. Point targets which experienced phase standard deviation below 0.65 radians were kept, leaving more than 115000 permanent scatterers.

The final solution was obtained by expanding the previous solution to more points of the data stack. This was achieved by interpolating the atmospheric contribution measured at the selected stable targets to the entire area of interest, thus obtaining the Atmospheric Phase Screen (APS). Linear regression was again tested against all the initial point candidates, leading to more permanent scatterers. Fig. 6 presents the deformation velocities obtained through the IPTA processing chain.

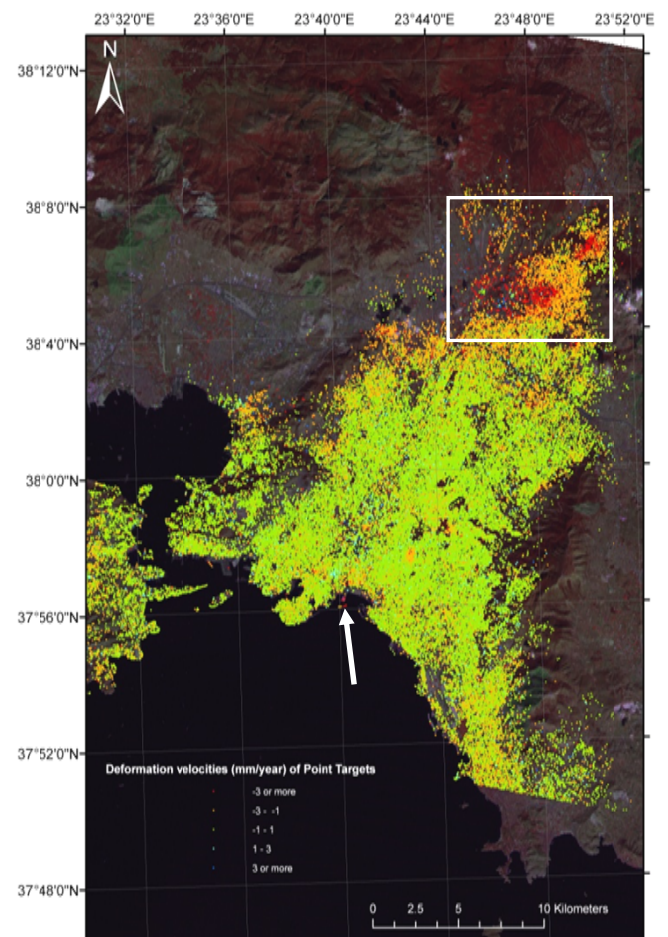


Figure 6. Deformation velocities in the Athens metropolitan area. Red points correspond to subsidence of 3 mm per year or more. The white box corresponds to the subsiding area of Kifissia.

The analysis generated also the actual elevation of the point scatterers, which usually differs from the corresponding DEM value, either due to SRTM errors or due to the fact that the target is not on the ground but probably mounted on a roof top of a building. Fig. 7 depicts the derived elevation of the permanent scatterers.

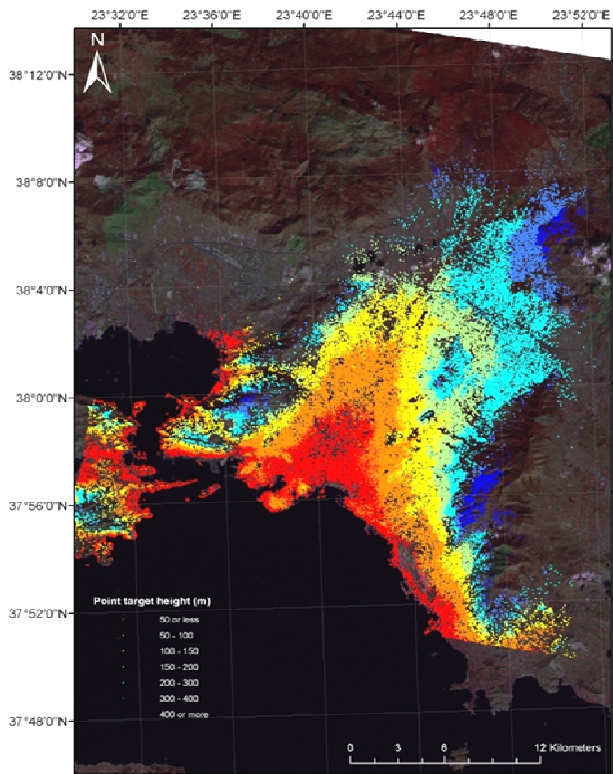


Figure 7. Elevation of the permanent scatterers in the Athens metropolitan area.

6. DISCUSSION OF THE RESULTS

The total number of accepted permanent scatterers was more 130000. The spatial density of the targets is considered very high, as it would be expected in an intensely urbanized area like the Athens metropolitan city.

The general deformation pattern in the area of this study shows weak deformation signal and is rather stable. Localised deformation signals are observed in certain boroughs of Athens (yellowish regions in Fig. 6) that are attributed to limited water pumping.

At the north-east of the scene though, in the area of Kifissia - a suburb of Athens, a strong displacement

signal is observed (white box in Fig. 6). This region exhibits deformation greater than 3 mm/year and up to 10 mm/year again attributed to intense water pumping. A close-up of part of Kifissia is shown in Fig. 8.



Figure 9. Permanent scatterers in part of the Kifissia subsiding area overlaid with a Google Earth background. The color coding is the same as in Fig. 6.

The white arrow on Fig. 9 is a target that is subsiding at a rate of 3.61 mm/year. The deformation history of this point is shown in Fig. 10. This point is not experiencing any non-linear deformation and the linear model fits well the interferometric data.

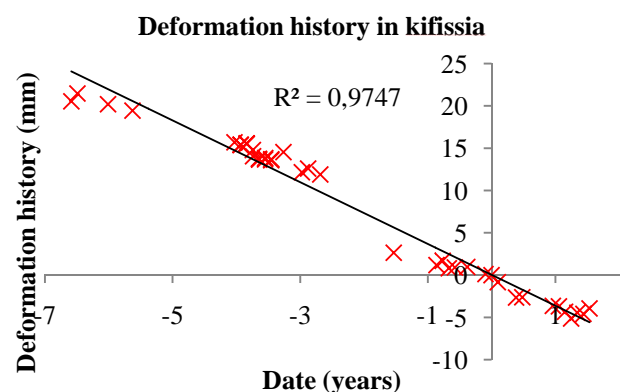


Figure 10. Deformation history for a selected point in Kifissia.

Another interesting scatterer is located on the south of the scene, in the port of Piraeus (white arrow in Fig. 6). The corresponding displacement history of this point is shown in Fig. 11.

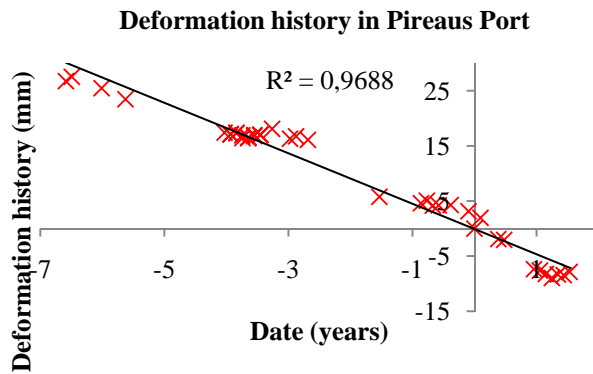


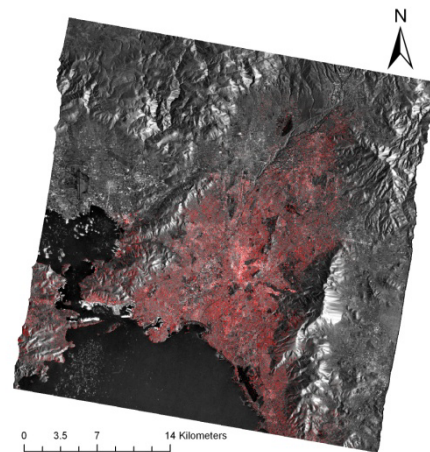
Figure 11. Deformation history for a selected point in Piraeus port.

Another interesting observation that is related to the algorithmic limitations of the method used is the lack of permanent scatterers at the north-west of Athens. This area is coinciding with the area that was affected by the 1999 Athens earthquake. This was not a simple non-linear deformation that extends over time, but a deformation step that occurred at one time instance. This was not accounted for in the model used for the interferometric phases, leading to large standard deviation values and hence these points were rejected as part of the thresholding procedure.

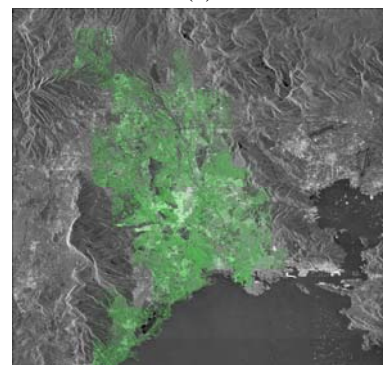
Finally it should be mentioned the deformation rates depicted in Fig.6 are consistent with those obtained within the TERRAFIRMA project, also presented in [6]. The validity of the results is further strengthened by the fact that in that analysis a completely different (and hence uncorrelated) dataset was used (adjacent track 236). The time span of the dataset used was from 1992 to 1999, prior to the Athens earthquake.

7. EXTENTION TO ENVISAT

As shown in section 3, 29 ENVISAT scenes have been acquired, of the same track and frame as the ERS dataset. For the time being, the same procedure as in the ERS case has been implemented, but exhaustive consistency checking of the derived products is unaccounted for and hence the results are not presented herein. It is however motivating to present the preliminary point scatterer density as opposed to the ERS scenario. This is shown in Fig. 12 where it is shown that the point target spatial coverage of the ENVISAT dataset coincides to a great extent with the ERS dataset.



(a)



(b)

Figure 12. Permanent scatterer density for the ERS dataset (a) and for the ENVISAT dataset.

8. CONCLUSIONS – FUTURE WORK

In the wider frame of a Greek collaboration scheme between the Institute for Space Applications and Remote Sensing of the National Observatory of Athens and the Dionysos Satellite Observatory of the National Technical University of Athens, aiming at the continuous monitoring of the Athens metropolitan area, some preliminary results were presented using the IPTA processing approach and ERS SAR data. Strong deformation signal was observed in the broader area of Kifissia, attributed to water pumping, along with some moderate displacement signals at other city locations. In addition the produced diachronic reference Point Target distribution map was a crucial step for the deployment of future validation schemes.

The planned progress of this work is focused on four main axes: (a) the inclusion of a model for the interferometric phases to account for the Athens earthquake, (b) the expansion of the solution to larger time spans, from 1992 to 2010, by including ENVISAT

acquisitions, (c) the derivation of the deformation rate by using all available ascending and descending datasets for the Athens metropolitan area and (d) the setup of a validation scheme with the use of an existing GPS network in the city of Athens and leveling campaigns.

9. REFERENCES

1. Kontoes, C.; Elias, P.; Sykioti, O.; Briole, P.; Remy, D.; Sachpazi, M.; Veis, G.; Kotsis, I. Displacement Field Mapping and Fault Modeling of the Mw = 5.9, September 7, 1999 Athens Earthquake based on ERS-2 Satellite RADAR Interferometry. *Geophysical Research Letters* **2000**, 27(24), 3989-3992.
2. Kotsis, I.; Kontoes, C.; Paradissis, D.; Karamitsos, S.; Elias, P.; Papoutsis, I. A methodology to Validate the InSAR Derived Displacement Field of the September 7th, 1999 Athens Earthquake Using Terrestrial Surveying. Improvement of the Assessed Deformation Field by Interferometric Stacking. *SENSORS* **2008**, 8(7), 4119-4134.
3. Kampes, B. M. RADAR INTERFEROMETRY, Persistent Scatterer Technique. *Springer* **2006**, pp 7.
4. Ferretti, A.; Prati, C.; Rocca, F. Permanent Scatterers in SAR Interferometry. *IEEE Trans. Geosci. Remote Sensing* **2001**, vol. 39, No. 1, 8–19.
5. GAMMA REMOTE SENSING. Interferometric Point Target Analysis User's Guide, <http://www.gamma-rs.ch/>
6. Parcharidis, I.; Lagios, E.; Sakkas, V.; Raucoules, D.; Fuerer, D.; Le Mouelic, S.; King, C.; Carnec, C.; Novali, F.; Ferretti, A.; Capes, R.; Cooksley, G. Subsidence Monitoring within the Athens Basin (Greece) Using Space Radar Interferometric Techniques. *Earth Planets Space* **2006**, 58, 505-513.